



Investigating neutron transfer in the ${}^6\text{Li} + {}^{124}\text{Sn}$ system

V. V. Parkar ^{1,2,*}, A. Parmar ³, Prasanna M.,⁴ V. Jha,^{1,2} and S. Kailas ⁵

¹*Nuclear Physics Division, Bhabha Atomic Research Centre, Mumbai 400085, India*

²*Homi Bhabha National Institute, Anushaktinagar, Mumbai 400094, India*

³*Department of Physics, Faculty of Science, The M. S. University of Baroda, Vadodara 390002, India*

⁴*Department of Physics, Rani Channamma University, Belagavi 591156, India*

⁵*UM-DAE Centre for Excellence in Basic Sciences, Mumbai 400098, India*



(Received 15 June 2022; revised 30 November 2022; accepted 27 January 2023; published 8 February 2023)

One-neutron stripping and pickup cross sections in the ${}^6\text{Li} + {}^{124}\text{Sn}$ system have been investigated through coupled-channel calculations by using a reliable global set of potentials. The systematics of one-neutron stripping and pickup cross sections with ${}^6\text{Li}$ projectiles on several targets have been presented. An approximate universal behavior is seen, which has been explained by a model based on barrier penetration. The neutron transfer along with cumulative sum of complete and incomplete fusion was found to explain most of the reaction cross section in the ${}^6\text{Li} + {}^{124}\text{Sn}$ system.

DOI: [10.1103/PhysRevC.107.024602](https://doi.org/10.1103/PhysRevC.107.024602)

I. INTRODUCTION

The investigation into mechanisms of reactions with weakly bound projectiles (WBPs) around Coulomb barrier energies has been a topic of intense interest in recent times. A variety of processes such as elastic scattering, complete and incomplete fusion, inclusive and exclusive breakup, and transfer have been studied in reactions using WBPs in this context [1,2]. In particular, the role of combined breakup and transfer processes and the extent to which they influence other processes have not been understood well. Breakup and transfer processes have been found to significantly affect other processes such as elastic scattering, α production, and complete and incomplete fusion [2].

The breakup process itself has been found to be predominantly triggered by nucleon transfer [3] in many cases. The neutron transfer process is of particular interest, which may be quite significant in many of the WBPs, which may lead to enhanced breakup of the projectile nucleus. The role of neutron transfer may also be crucial in the context of explaining the copious α emission for ${}^{6,7}\text{Li}$ projectiles measured at energies around the Coulomb barrier. The breakup process driven by neutron transfer may provide the additional source of α production in these reactions. In addition, neutron transfer channels are also expected to provide important coupling effects that may be necessary to explain the fusion behavior for these systems at energies around the Coulomb barrier. Therefore, a comprehensive understanding of neutron transfer and its relation to other reaction processes is very crucial.

The neutron transfer reactions, besides their role in overall breakup of the projectile and inclusive α production is necessary for understanding several other related features, such

as enhanced reaction and incomplete fusion cross sections. While conventionally it is well accepted that neutron transfer may provide additional fusion enhancement at below-barrier energies, the situation with WBPs may be the reverse in some situations. The neutron transfer processes may also be reason for suppression of the fusion cross sections at energies above the barrier. In many systems, the $1n$ transfer to target continuum states is the dominant contribution to the ICF process.

Theoretical modeling of these processes is easier for the noncapture breakup (NCBU) process (refers to processes in which, in principle, both projectile fragments, e.g., α and d in ${}^6\text{Li}$ breakup, survive and can be measured) and transfer to low-lying discrete states. For example, continuum discretized coupled-channel (CDCC) and coupled reaction channel (CRC) calculations, respectively, can be employed to describe these processes reasonably well. However, the complexity increases if the breakup process is followed by absorption of one of the fragments leading to breakup fusion [4,5] or the transfer takes place to the high-lying states of the target [6,7] both below and above the particle emission thresholds. Moreover, the description of sequential two-step processes such as the transfer-induced breakup is highly non-trivial.

In our earlier work with ${}^7\text{Li}$ projectiles on several targets, $1n$ stripping and $1n$ pickup cross sections are shown to follow a universal behavior [8]. Also, a crucial aspect of $1n$ transfer is its onset as compared with other reaction channels at energies around the barrier. Apart from $1n$ stripping, which contributes significantly, many other reaction channels such as proton transfer, NCBU, and target inelastic states were found to be necessary for a complete explanation. In contrast, for the ${}^6\text{Li}$ nucleus, while the breakup and processes assisted by it are expected to be dominant, so other channels may have a relatively weaker role.

In the present work, the mechanisms of $1n$ stripping and pickup cross sections measured in the ${}^6\text{Li} + {}^{124}\text{Sn}$ system

*Corresponding author: vparkar@barc.gov.in

TABLE I. Optical model potential parameters used in CRC1 calculations. The radius parameter in the potentials are derived from $R_i = r_i A_T^{1/3}$, where $i = R, V, S, C$ and A is the target mass number

System	V_R (MeV)	r_R (fm)	a_R (fm)	W_V (MeV)	r_V (fm)	a_V (fm)	W_S (MeV)	r_S (fm)	a_S (fm)	r_C (fm)	Ref.
${}^6\text{Li} + {}^{124}\text{Sn}$	259.2	1.12	0.81	0.10	1.54	0.73	12.00 ^a	1.31	0.94	1.67	[11]
${}^7\text{Li} + {}^{123}\text{Sn}$	179.9	1.24	0.85	22.22	1.59	0.60	36.01	1.18	0.87	1.80	[12]

^aThis depth is optimum to fit the elastic scattering data at all the energies.

[9] have been investigated. CRC calculations have been performed to understand the mechanisms of both $1n$ stripping and $1n$ pickup reactions. Generally these calculations have shown ambiguities with respect to the choice of optical model parameters. To avoid this, a well-tested global set of potentials has been employed for the calculations. For estimating NCBU cross sections, CDCC calculations have also been performed. These processes are found to affect the elastic scattering and the fusion cross sections. Furthermore, the systematic behavior of $1n$ transfer data measured for various targets using ${}^6\text{Li}$ projectiles has been investigated.

The paper is organized as follows: Calculation details are given in Sec. II. The results are discussed in Sec. III, and a summary is given in Sec. IV.

II. CALCULATION DETAILS

Coupled-channel calculations have been performed to understand the mechanisms related to transfer and breakup reactions. In particular, we focus on the role of neutron transfer through these calculations. For completeness, four kinds of calculations, namely, (i) CRC using phenomenological global optical model potentials (CRC1), (ii) CRC using normalized microscopic São Paulo potentials (CRC2), (iii) CDCC, and (iv) combined CDCC + CRC have been performed. These calculations have been performed using the code FRESKO (version FRES 2.9) [10]. The elastic scattering, NCBU, and $1n$ transfer cross sections have been calculated. The detailed discussion on the calculation procedure was given in our earlier paper [8]. Here we discuss it only briefly.

A. Coupled reaction channel calculations

CRC (type 1) calculations (CRC1) have been performed by using the global phenomenological optical model potentials for ${}^6\text{Li} + {}^{124}\text{Sn}$ [11] in the entrance and exit channel for $1n$ stripping process. For the $1n$ pickup reactions, the same potential for ${}^6\text{Li} + {}^{124}\text{Sn}$ [11] in the entrance and the ${}^7\text{Li} + {}^{124}\text{Sn}$ [12] potential in the exit channel was used. The potential parameters are given in Table I. The potentials binding the transferred particles were of the Woods-Saxon volume form, with radius $1.25A^{1/3}$ fm and diffuseness 0.65 fm, with “ A ” being the mass of the core nucleus. The depths were adjusted to obtain the required binding energies of the particle-core composite system. The single-particle states along with spectroscopic factors (C^2S) for the residual nuclei (${}^{123}\text{Sn}$ and ${}^{125}\text{Sn}$) considered in the calculations were given in Table I of Ref. [8]. For the ${}^6\text{Li} + n \rightarrow {}^7\text{Li}$ transfer, both the $1p_{3/2}$ and $1p_{1/2}$ components of the neutron bound to ${}^6\text{Li}$ were included with spectroscopic factors of $C^2S = 0.43$ and 0.29 ,

respectively [13,14], taken from Cohen and Kurath [15]. Similarly for the ${}^6\text{Li} \rightarrow {}^5\text{Li} + n$ transfer, the $1p_{3/2}$ component of the neutron bound to ${}^5\text{Li}$ was included with spectroscopic factor of $C^2S = 1.12$ [16]. The finite-range form factors in the post form for stripping and prior form for pickup were used. Calculations were carried out including the full complex remnant term.

CRC (type 2) calculations (CRC2) are similar to CRC1 except for the use of microscopic double-folding São Paulo potentials (SPPs) [17,18] for real and imaginary parts of the optical potential. In the incoming partitions, the strength coefficients for real and imaginary potentials were kept as $N_R = N_I = 0.6$, as adopted in previous works [8,19–23] to account for the loss of flux to dissipative and breakup channels [19,20] and repulsive nature of the real part of the breakup polarization potential [21,24–30]. In the outgoing partition, the SPP was used for both the real and the imaginary parts with strength coefficients $N_R = 1.0$ and $N_I = 0.78$ [31], respectively.

B. CDCC and CDCC + CRC calculations

To investigate the effect of projectile breakup and neutron transfer on elastic scattering as well as for estimating the breakup and transfer cross sections simultaneously, the CDCC and combined CDCC + CRC calculations have been carried out. Both the inelastic excitations of the projectile and neutron transfer channels have been coupled.

The coupling scheme used in CDCC is similar to that described in earlier works [4,27,29]. In the calculations, the cluster structure of ${}^6\text{Li} \rightarrow \alpha + d$ ($E_{\text{thres}} = 1.47$ MeV) was assumed. The continuum above the E_{thres} was discretized into bins of constant momentum width $k = 0.20$ fm⁻¹, where $\hbar k$ is the momentum of $\alpha + d$ relative motion. The coupling states with relative orbital angular momentum $L = 0, 1, 2, 3$ and $1^+, 2^+,$ and 3^+ resonances were included in the calculation. The binding potential for $\alpha - d$ in ${}^6\text{Li}$ was taken from Ref. [32]. The real and imaginary parts of required fragment-target potentials $V_{\alpha-T}$ and V_{i-T} in the cluster folding model were taken from the São Paulo potential [18] with strength 1.0 and 0.78, respectively. In addition to CDCC calculations for breakup, the CRC calculations of type CRC1 and CRC2, as explained above, were simultaneously performed. These calculations were done by considering CDCC coupling from the ${}^6\text{Li}$ ground state to the ${}^6\text{Li}$ excited states but still considering that the transfer happens only from the ground state of ${}^6\text{Li}$ to the ground state of ${}^5,7\text{Li}$. These states are not strictly orthogonal, as a low energy $d + \alpha$ continuum state may overlap with a ${}^5\text{Li} + n$ configuration that undergoes transfer.

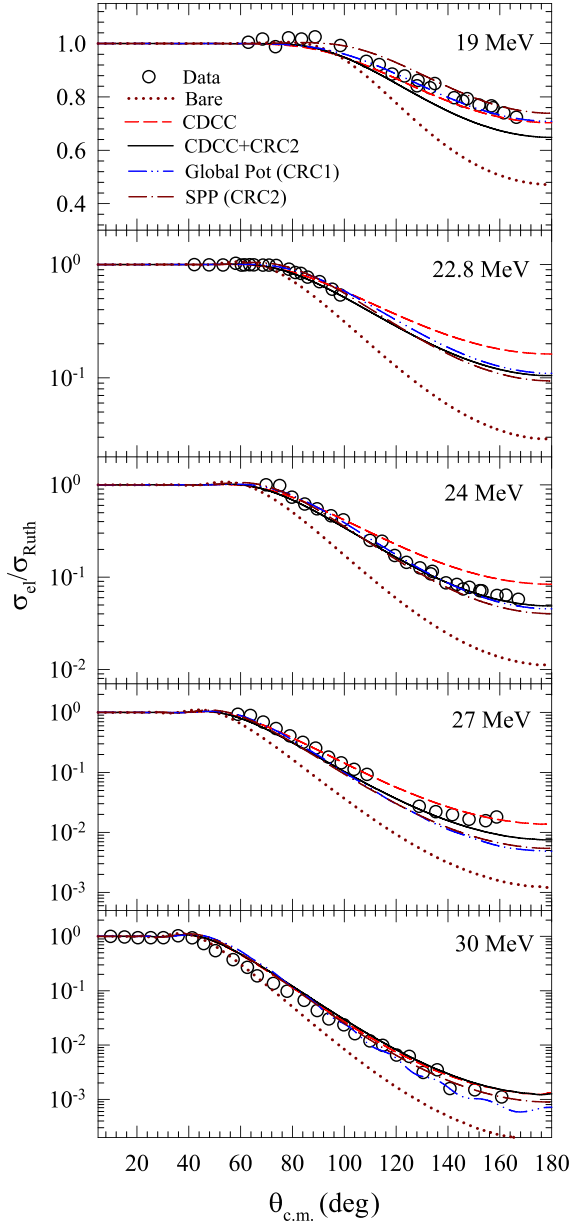


FIG. 1. Elastic scattering data for the ${}^6\text{Li} + {}^{120}\text{Sn}$ system [11,33,34] are compared with the calculations performed for ${}^6\text{Li} + {}^{124}\text{Sn}$ system (see text for details).

III. RESULTS AND DISCUSSION

A. Elastic scattering

The elastic scattering data available for the ${}^6\text{Li} + {}^{120}\text{Sn}$ system at 19, 24, 27 MeV [33], 22.8 MeV [34], and 30 MeV [11] was utilized for testing our entrance channel potentials and also to see the effect of breakup and neutron transfer couplings on the elastic scattering angular distributions. It is to be noted that all the calculations were done for the ${}^6\text{Li} + {}^{124}\text{Sn}$ system, however, the elastic scattering data of the ${}^6\text{Li} + {}^{120}\text{Sn}$ system was used as a proxy for the not-yet-measured ${}^6\text{Li} + {}^{124}\text{Sn}$ system because we do not expect considerable difference in elastic scattering. A similar thing

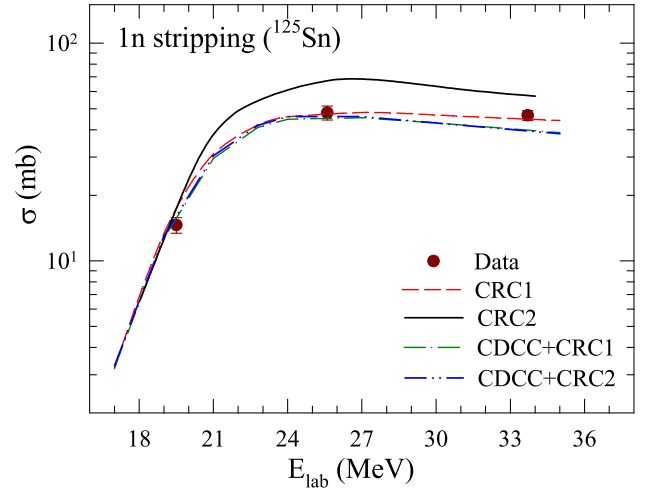


FIG. 2. Measured $1n$ stripping cross sections in the ${}^6\text{Li} + {}^{124}\text{Sn}$ system are compared with the four set of calculations (see text for details).

was demonstrated for ${}^7\text{Li} + {}^{120}\text{Sn}$ and ${}^7\text{Li} + {}^{124}\text{Sn}$ systems at 28 MeV in Ref. [8]. The elastic scattering data and the calculations are compared in Fig. 1. The calculated elastic scattering angular distributions using global potential (used in CRC1) and using SPP (used in CRC2) are shown with dashed-dot-dotted and dashed-dotted lines, respectively. Both the calculations agree with the data very well. The calculations with CDCC and CDCC + CRC2 are also shown as dashed and solid lines, respectively. CDCC + CRC1 calculations are not shown here as they are similar to CDCC + CRC2 calculations and hence difficult to distinguish. Dotted lines are the calculations with bare potential without including any continuum couplings. It can be seen that the coupling of the breakup channel has a significant effect on elastic scattering. A similar observation is also pointed out in previous works [27,29]. With the inclusion of transfer channel, the elastic scattering cross sections are only slightly changed indicating the effect of breakup couplings is much more than the transfer couplings.

B. $1n$ stripping and $1n$ pickup

The $1n$ stripping data leading to ${}^{125}\text{Sn}$ residual nucleus was measured by offline γ -ray counting and reported in Ref. [9]. The ground-state Q value for n stripping for this reaction is 0.07 MeV. The calculations of CRC (CRC1, CRC2), CDCC + CRC1, and CDCC + CRC2 type are compared with the data in Fig. 2. As depicted in Fig. 2, the results from all the calculations agree very well with the data, except that CRC2 shows slight overprediction above 19 MeV.

Similar to the $1n$ stripping channel, the data for $1n$ pickup leading to ${}^{123}\text{Sn}$ residual nucleus (only m.s. state) were also measured in Ref. [9]. The ground-state Q value for n pickup for this reaction is -1.24 MeV. The calculations of CRC (CRC1, CRC2), CDCC + CRC1, and CDCC + CRC2 type are compared with the measured data in Fig. 3. The CRC2 calculation shows a slight overprediction with respect to the data, while the CRC1 and CDCC + CRC calculations agree with

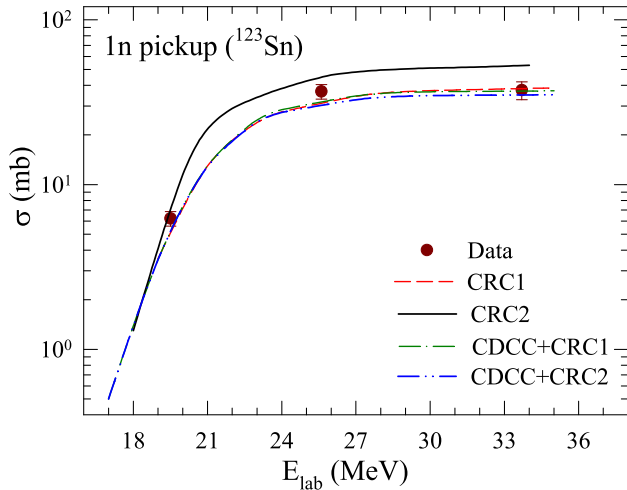


FIG. 3. Measured $1n$ pickup cross sections in the ${}^6\text{Li} + {}^{124}\text{Sn}$ system are compared with the four set of calculations (see text for details).

the data. The ${}^{123}\text{Sn}$ residual nucleus may have the contribution from $1p$ pickup also as pointed out in our earlier work with ${}^7\text{Li}$ [8]. However, as the ground-state Q value for p pickup with ${}^6\text{Li}$ projectiles is -6.49 MeV, this route for production of ${}^{123}\text{Sn}$ is expected to be insignificant.

C. Systematics of neutron transfer cross sections with ${}^6\text{Li}$ projectile

The data available for $1n$ stripping and $1n$ pickup cross sections with ${}^6\text{Li}$ projectile on ${}^{27}\text{Al}$ [35], ${}^{96}\text{Zr}$ [22], ${}^{124}\text{Sn}$ [9], ${}^{159}\text{Tb}$ [36], ${}^{197}\text{Au}$ [37], ${}^{198}\text{Pt}$ [38] targets are plotted in Figs. 4(a) and 4(b). Here, the variable on the X axis is chosen to remove any geometrical factors due to target size. The universal behavior in the cross sections in both the plots was observed. The transfer systematics in Figs. 4(a) and 4(b) are interesting and are presented with the ${}^6\text{Li}$ projectile. Similar systematic have also been observed with the ${}^7\text{Li}$ [8] and

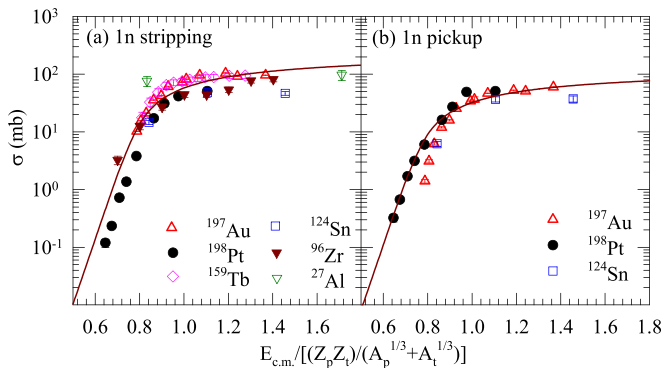


FIG. 4. Systematic behavior of (a) $1n$ stripping, and (b) $1n$ pickup cross sections as a function of reduced energy with ${}^6\text{Li}$ projectile on various targets. The transfer cross-section data available for ${}^{27}\text{Al}$ [35], ${}^{96}\text{Zr}$ [22], ${}^{124}\text{Sn}$ [9], ${}^{159}\text{Tb}$ [36], ${}^{197}\text{Au}$ [37], ${}^{198}\text{Pt}$ [38] targets were utilized. Lines are fits to the data.

TABLE II. a and c values obtained from the fitting of the universal plots of Fig. 4.

Process	S_n (MeV)	a (MeV)	c (MeV^{-1})
(a) $1n$ stripping	5.66	-4.62	0.45
(b) $1n$ pickup	7.25	-4.92	0.44

with the ${}^9\text{Be}$ projectile [23,39]. To explain the appearance of universal behavior in these plots [Figs. 4(a) and 4(b)], we have used the Wong formula [40], which is based on the barrier penetration, as done in Ref. [8]. The expression of the Wong formula has been modified and multiplied by transfer probability $[\exp(-cS_n)]$ as given below:

$$\sigma = \frac{\hbar\omega}{2E_{c.m.}} R_b^2 \log \left[1 + \exp \left(\frac{2\pi}{\hbar\omega} (E_{c.m.} - V_b - a) \right) \right] \times \exp(-cS_n), \quad (1)$$

where a and c are the parameters which were varied to fit the data. S_n are the separation energies for $1n$ stripping or pickup. The parameter “ a ” represents the shift in the barrier for the specific reaction channel, while the parameter “ c ” provides the overall normalization to describe the transfer cross section in magnitude. The values of V_b , R_b , and $\hbar\omega$ for the ${}^6\text{Li} + {}^{124}\text{Sn}$ system were taken from Ref. [9]. The resulting fits are shown as the solid lines in Figs. 4(a) and 4(b). The values of a and c that have been obtained are given in Table II. The values of parameter “ a ” explains the early onset of these transfer processes as compared with the nominal barrier as observed in data. The “ a ” parameter is similar for both neutron stripping and pickup data. This is consistent with the S_n values being similar for the two processes. It is to be noted that the “ a ” parameter in neutron stripping data for ${}^7\text{Li}$ is also similar [8], consistent with S_n value. This parameter can be related to the barrier position minus threshold energy (B-T value) evaluated from the fusion data using the Stelson model [41]. This is certainly not the case in neutron transfer cross sections of deuterons [42], in which the drop of the fusion cross section is much faster, below the barrier, than the drop in neutron transfer.

D. Reaction mechanism in the ${}^6\text{Li} + {}^{124}\text{Sn}$ system

To understand the complete reaction mechanism in the ${}^6\text{Li} + {}^{124}\text{Sn}$ system, the measured CF, ICF, total fusion (TF), neutron transfer cross sections [9], and their sum are compared with the deduced reaction cross sections from the present calculations, shown in Fig. 5. The reaction cross sections obtained from the global optical model potential of Ref. [11], from SPP and from CDCC are found to be similar (within 10%). It also shows the fusion cross sections calculated in CDCC by the barrier penetration model (BPM) using the bare potential, which reproduces the experimental TF at above-barrier energies but underpredict it at subbarrier energies. The cumulative absorption cross sections from CDCC + CRC calculations are found to agree with the sum of TF and $1n$ transfer cross sections. NCBU cross sections from CDCC calculations are also shown, which has

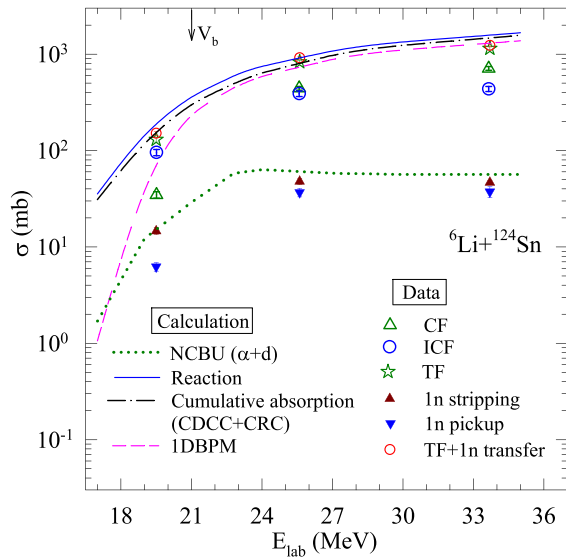


FIG. 5. Measured CF, ICF, transfer cross sections [9] and their sum are compared with the reaction cross sections. NCBU, cumulative absorption, and BPM model calculations are also shown (see text for details).

lower contributions compared with CF and ICF cross sections. The possible minor contributions to the reaction cross sections from other channels such as proton transfer, NCBU, and target inelastic states were not measured.

IV. SUMMARY

In summary, we have investigated the importance of neutron transfer and breakup in the ${}^6\text{Li} + {}^{124}\text{Sn}$ system at energies around the Coulomb barrier. CRC calculations for $1n$

stripping and $1n$ pickup have been performed by using the global optical model potential parameters as well as by using the São Paulo potential for the ${}^6\text{Li} + {}^{124}\text{Sn}$ system. The elastic scattering data of ${}^6\text{Li} + {}^{120}\text{Sn}$ was used to test our entrance channel potentials. CDCC and CDCC + CRC calculations have also been performed to investigate the combined effects of breakup and transfer channels. For the CDCC calculations, the bare potential used was obtained from folding the São Paulo potential of $\alpha + {}^{124}\text{Sn}$ and $d + {}^{124}\text{Sn}$ systems. The CDCC + CRC calculations provide a reasonably good description of elastic scattering, $1n$ stripping, $1n$ pickup, and total fusion processes for a system involving ${}^6\text{Li}$ projectiles in an effective but approximate way. Universal behavior of stripping and pickup cross sections with ${}^6\text{Li}$ projectiles on several targets was established. An early onset of the neutron transfer compared with fusion reactions is seen. This feature is important in context of relative competition of different reaction processes around the Coulomb barrier. Similar observation is reported in earlier study with the ${}^7\text{Li}$ projectile. The cumulative of measured CF, ICF, along with $1n$ transfer cross sections almost explain the estimated reaction cross section for the ${}^6\text{Li} + {}^{124}\text{Sn}$ system. Furthermore, it has been found that $1n$ transfer is one of the important contributor to α production in ${}^6,7\text{Li}$ -induced reactions. Similar studies of contribution of neutron transfer in α production with other projectiles will be interesting.

ACKNOWLEDGMENTS

The authors V.V.P. and S.K. acknowledge the financial support from the Young Scientist Research grant and Senior Scientist programme, respectively, and from the Indian National Science Academy (INSA), Government of India, in carrying out these investigations.

-
- [1] L. F. Canto, P. R. S. Gomes, R. Donangelo, J. Lubian, and M. S. Hussein, *Phys. Rep.* **596**, 1 (2015).
- [2] V. Jha, V. V. Parkar, and S. Kailas, *Phys. Rep.* **845**, 1 (2020), and references therein.
- [3] D. H. Luong, M. Dasgupta, D. J. Hinde, R. du Rietz, R. Rafiei, C. J. Lin, M. Evers, and A. Diaz-Torres, *Phys. Rev. C* **88**, 034609 (2013).
- [4] V. V. Parkar, V. Jha, and S. Kailas, *Phys. Rev. C* **94**, 024609 (2016).
- [5] J. Lubian, J. L. Ferreira, J. Rangel, M. R. Cortes, and L. F. Canto, *Phys. Rev. C* **105**, 054601 (2022).
- [6] A. M. Moro and F. M. Nunes, *Nucl. Phys. A* **767**, 138 (2006).
- [7] J. P. Fernández-García, M. A. G. Alvarez, A. M. Moro, and M. Rodríguez-Gallardo, *Phys. Lett. B* **693**, 310 (2010).
- [8] V. V. Parkar, A. Parmar, P. M., V. Jha, and S. Kailas, *Phys. Rev. C* **104**, 054603 (2021).
- [9] V. V. Parkar, S. K. Pandit, A. Shrivastava, R. Palit, K. Mahata, V. Jha, K. Ramachandran, S. Gupta, S. Santra, S. K. Sharma, S. Upadhyaya, T. N. Nag, S. Bhattacharya, T. Trivedi, and S. Kailas, *Phys. Rev. C* **98**, 014601 (2018).
- [10] I. J. Thompson, *Comput. Phys. Rep.* **7**, 167 (1988).
- [11] Y. Xu, Y. Han, J. Hu, H. Liang, Z. Wu, H. Guo, and C. Cai, *Phys. Rev. C* **98**, 024619 (2018).
- [12] Y. Xu, Y. Han, J. Hu, H. Liang, Z. Wu, H. Guo, and C. Cai, *Phys. Rev. C* **97**, 014615 (2018).
- [13] P. Schumacher, N. Ueta, H. H. Duhm, K. I. Kubo, and W. J. Klages, *Nucl. Phys. A* **212**, 573 (1973).
- [14] J. Cook, *Nucl. Phys. A* **388**, 153 (1982).
- [15] S. Cohen and D. Kurath, *Nucl. Phys. A* **101**, 1 (1967).
- [16] M. B. Tsang, J. Lee, and W. G. Lynch, *Phys. Rev. Lett.* **95**, 222501 (2005).
- [17] L. C. Chamon, D. Pereira, M. S. Hussein, M. A. Cândido Ribeiro, and D. Galetti, *Phys. Rev. Lett.* **79**, 5218 (1997).
- [18] L. C. Chamon, B. V. Carlson, L. R. Gasques, D. Pereira, C. De Conti, M. A. G. Alvarez, M. S. Hussein, M. A. Cândido Ribeiro, E. S. Rossi, and C. P. Silva, *Phys. Rev. C* **66**, 014610 (2002).
- [19] D. Pereira, J. Lubian, J. R. B. Oliveira, D. P. de Sousa, and L. C. Chamon, *Phys. Lett. B* **670**, 330 (2009).
- [20] D. P. Sousa, D. Pereira, J. Lubian, L. C. Chamon, J. R. B. Oliveira, E. S. Rossi, C. P. Silva, P. N. de Faria, V. Guimarães, R. Lichtenthaler *et al.*, *Nucl. Phys. A* **836**, 1 (2010).
- [21] Y. Sakuragi, M. Yahiro, and M. Kamimura, *Prog. Theor. Phys.* **70**, 1047 (1983).

- [22] S. P. Hu, G. L. Zhang, J. C. Yang, H. Q. Zhang, P. R. S. Gomes, J. Lubian, J. L. Ferreira, X. G. Wu, J. Zhong, C. Y. He *et al.*, *Phys. Rev. C* **93**, 014621 (2016).
- [23] Y. D. Fang, P. R. S. Gomes, J. Lubian, J. L. Ferreira, D. R. Mendes Junior, X. H. Zhou, M. L. Liu, N. T. Zhang, Y. H. Zhang, G. S. Li *et al.*, *Phys. Rev. C* **93**, 034615 (2016).
- [24] M. Kamimura, M. Yahiro, Y. Iseri, Y. Sakuragi, H. Kameyama, and M. Kawai, *Prog. Theor. Phys. Suppl.* **89**, 1 (1986).
- [25] Y. Sakuragi, *Phys. Rev. C* **35**, 2161 (1987).
- [26] R. S. Mackintosh and N. Keeley, *Phys. Rev. C* **79**, 014611 (2009).
- [27] H. Kumawat, V. Jha, B. J. Roy, V. V. Parkar, S. Santra, V. Kumar, D. Dutta, P. Shukla, L. M. Pant, A. K. Mohanty *et al.*, *Phys. Rev. C* **78**, 044617 (2008).
- [28] V. V. Parkar, I. Martel, A. M. Sánchez-Benítez, L. Acosta, K. Rusek, Ł. Standylo, and N. Keeley, *Acta Phys. Pol., B* **42**, 761 (2011).
- [29] S. Santra, S. Kailas, K. Ramachandran, V. V. Parkar, V. Jha, B. J. Roy, and P. Shukla, *Phys. Rev. C* **83**, 034616 (2011).
- [30] V. V. Parkar, V. Jha, S. K. Pandit, S. Santra, and S. Kailas, *Phys. Rev. C* **87**, 034602 (2013).
- [31] L. R. Gasques, M. Dasgupta, D. J. Hinde, T. Peatey, A. Diaz-Torres, and J. O. Newton, *Phys. Rev. C* **74**, 064615 (2006).
- [32] K. I. Kubo and M. Hirata, *Nucl. Phys. A* **187**, 186 (1972).
- [33] M. A. G. Alvarez, J. P. Fernández-García, J. L. León-García, M. Rodríguez-Gallardo, L. R. Gasques, L. C. Chamon, V. A. B. Zagatto, A. Lépine-Szily, J. R. B. Oliveira, V. Scarduelli *et al.*, *Phys. Rev. C* **100**, 064602 (2019).
- [34] V. Chuev, Y. Glukhov, V. Manko, B. Novatskii, A. Ogloblin, S. Sakuta, and D. Stepanov, *Phys. Lett. B* **42**, 63 (1972).
- [35] I.-M. Ladenbauer, I. L. Preiss, and C. E. Anderson, *Phys. Rev.* **123**, 1368 (1961).
- [36] M. K. Pradhan, A. Mukherjee, Subinit Roy, P. Basu, A. Goswami, R. Kshetri, R. Palit, V. V. Parkar, M. Ray, M. Saha Sarkar *et al.*, *Phys. Rev. C* **88**, 064603 (2013).
- [37] C. S. Palshetkar, Shital Thakur, V. Nanal, A. Shrivastava, N. Dokania, V. Singh, V. V. Parkar, P. C. Rout, R. Palit, R. G. Pillay *et al.*, *Phys. Rev. C* **89**, 024607 (2014).
- [38] A. Shrivastava, A. Navin, A. Diaz-Torres, V. Nanal, K. Ramachandran, M. Rejmund, S. Bhattacharyya, A. Chatterjee, S. Kailas, A. Lemasson *et al.*, *Phys. Lett. B* **718**, 931 (2013).
- [39] Malika Kaushik, S. K. Pandit, V. V. Parkar, G. Gupta, S. Thakur, V. Nanal, H. Krishnamoorthy, A. Shrivastava, C. S. Palshetkar, K. Mahata *et al.*, *Phys. Rev. C* **104**, 024615 (2021).
- [40] C. Y. Wong, *Phys. Rev. Lett.* **31**, 766 (1973).
- [41] P. H. Stelson, H. J. Kim, M. Beckerman, D. Shapira, and R. L. Robinson, *Phys. Rev. C* **41**, 1584 (1990).
- [42] M. Avrigeanu, E. Šimečková, U. Fischer, J. Mrázek, J. Novak, M. Štefánik, C. Costache, and V. Avrigeanu, *Phys. Rev. C* **94**, 014606 (2016), and references therein.